

## ESR Studies of Copper(II) Ion Doped in Single Crystal of Benzo-15-crown-5 Complex

Yong LI, Kunihiro TAJIMA, Kazuhiko ISHIZU,\* and Nagao AZUMA†  
 Department of Chemistry, Faculty of Science, Ehime University, Matsuyama 790  
 †Faculty of General Education, Ehime University, Matsuyama 790  
 (Received February 6, 1988)

Angular-dependent ESR measurements were carried out at 77 K for  $^{65}\text{Cu(II)}$  ions doped in a single crystal of benzo-15-crown-5 (B15C5) magnesium complex. Not only the allowed resonance lines of copper(II) ions, but also the forbidden lines arising from a nuclear quadrupole interaction were observed. Based on an analysis of the single crystal ESR spectra, the spin Hamiltonian containing the quadrupole term was determined for a B15C5- $^{65}\text{Cu(II)}$  complex having a  $3d_{z^2}$  ground state in a B15C5-Mg(II) solid matrix.

Regarding previous work, we have reported ESR studies on copper(II) complexes with 15-crown-5 (15C5) derivatives in solution,<sup>1)</sup> where the benzo-15-crown-5-copper(II) complexes (B15C5-Cu(II)) revealed the characteristic ESR  $g$ -anisotropies ( $g_z < g_x, g_y$ ) which are typical of the copper(II) ion with a  $3d_{z^2}$  ground-state doublet. In the ESR spectra measured in solution, however, the full Hamiltonian involving the nuclear quadrupole interaction could not be determined.

In the present paper, we report on the ESR spectra observed at 77 K for a B15C5- $^{65}\text{Cu(II)}$  complex doped in a diamagnetic single crystal composed of a benzo-15-crown-5-Mg(II) complex. The copper(II) complex also exhibited the inverse  $g$ -values ( $g_z < g_x, g_y$ ) featured by the  $3d_{z^2}$  ground state. In addition, strong lines due to a forbidden transition of the copper(II), ascribed to a quadrupole interaction, were successfully observed for the  $3d_{z^2}$  ground state. An analysis of the angular-dependent ESR spectra determined the magnitude of the nuclear quadrupole interaction, which would be affected by a strong axial perturbation in the present complex.

### Experimental

B15C5 was prepared according to Pedersen's method.<sup>2)</sup>  $\text{Mg}(\text{ClO}_4)_2 \cdot 6\text{H}_2\text{O}$  and 60%- $\text{HClO}_4$  were purchased.

In order to obtain a B15C5-Mg(II) single crystal doped with copper(II),  $^{65}\text{CuSO}_4 \cdot 5\text{H}_2\text{O}$  was added to a  $0.5 \text{ mol dm}^{-3}$  60%- $\text{HClO}_4$  solution of B15C5 and  $\text{Mg}(\text{ClO}_4)_2 \cdot 6\text{H}_2\text{O}$  mixed in an equivalent molar ratio, in which the  $^{65}\text{Cu(II)}$  concentration was controlled to be 1% of the total Mg(II) concentration. The mixture was left standing for one week, after which yellow single crystals were obtained.

A doped single crystal was mounted on the plane of a goniometer rod with silicone grease. The single crystal ESR spectra were recorded at 77 K. Figure 1 (a) illustrates the relation between the magnetic field  $H$  and the coordinate systems used. The coordinate systems,  $(0\text{-}xyz)$  and  $(0\text{-}123)$ , represent those fixed to the goniometer and to the single crystal, respectively. By appropriate intervals in the  $\phi$  angle, the crystal was rotated around the  $z$ -axis (Fig. 1(a)) with  $\alpha = 2.8^\circ$  and  $18.2^\circ$  being adopted. The direction of the magnetic field  $H$  is taken in the  $x$ - $y$  plane. Figure 1 (b)

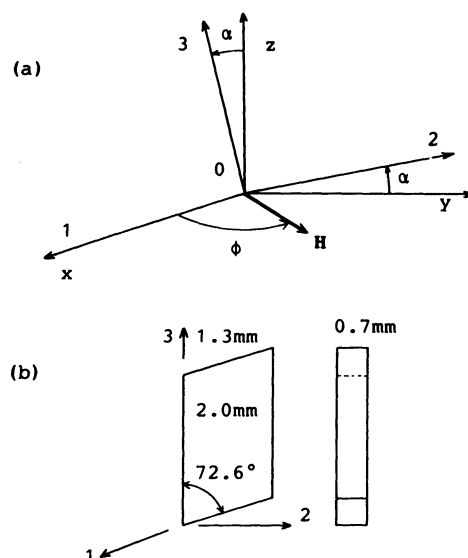


Fig. 1. (a) Coordinate systems adopted in the ESR measurement. The systems  $(0\text{-}xyz)$  and  $(0\text{-}123)$  were fixed to the goniometer and to the crystal, respectively. The crystal is mounted on the  $y$ - $z$  plane, with keeping the axis 1 parallel to the  $x$  axis, and  $\alpha$  is the angle between the axes 3 and  $z$ . The crystal is rotated around the  $z$  axis, so the magnetic field  $H$  is also rotated in the  $x$ - $y$  plane by  $\phi$  angle. (b) The arrangement of the  $(0\text{-}123)$  coordinate system in the single crystal with its dimension.

shows the arrangement of the  $(0\text{-}123)$  coordinate system in the single crystal with its dimensions.

The ESR measurements were carried out on a JEOL-FX-2XG X-band ESR spectrometer operating with a 100-kHz magnetic-field modulation. The positions of the resonance lines were determined by taking Li-TCNQ ( $g = 2.0025$ ) as a standard. The magnetic fields were calibrated based on the hyperfine splitting of Mn(II) in powdered MgO (8.69 mT).

### Results and Discussion

Figure 2 (a) shows the powder ESR spectrum observed at room temperature. The spectrum revealed a typical  $g$ -anisotropy,  $g_z < g_x, g_y$ , which was similar to that of a B15C5-copper(II) complex also having a  $3d_{z^2}$

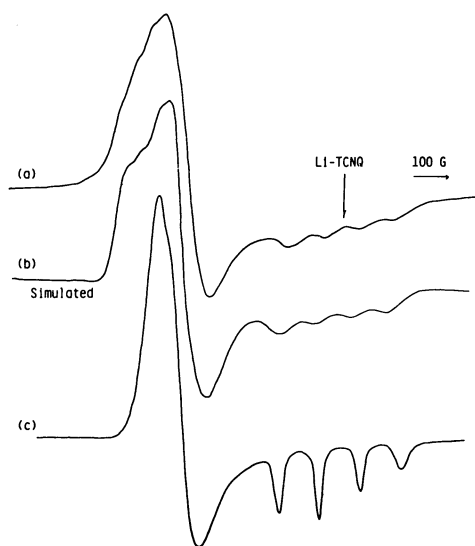


Fig. 2. Powder ESR spectrum of  $^{65}\text{Cu}(\text{II})$  doped in the crystal of B15C5-Mg(II) complex, measured at room temperature (a) and its simulation (b). Spectrum (c) was obtained from the B15C5- $^{65}\text{Cu}(\text{II})$  complex in 60%-HClO<sub>4</sub> aqueous solution at 77 K.

ground state in solution (Fig. 2(c)).

Figures 3 and 4 show the angular-dependent ESR spectra of the  $^{65}\text{Cu}(\text{II})$  doped in a single crystal. The eight lines marked with asterisks and arrows have been assigned to the allowed transitions in two magnetically unequivalent copper sites. The other lines are ascribed to the forbidden transition ( $\Delta M_I = \pm 1$ ). However, the range of the rotation angle ( $\phi$ ), in which one could observe each of those forbidden lines, has been very small. This is because the hindrance by the much stronger eight allowed lines and the overlapping between the forbidden transition lines themselves are inevitable. Therefore, an analysis of the angular variation of the forbidden lines has been almost impossible. We therefore confined our spectral analysis to only the allowed lines. In a usual case, the forbidden transition of copper(II) ion can not be detected in the X-band ESR spectra, because of its small transition probability. Thus, information concerning the quadrupole coupling is usually obtained from the Q-band ESR spectra for a single crystal.<sup>3)</sup> Here, it is quite noteworthy that the forbidden lines were observed, even in the X-band spectra. This indicates that the probability of a forbidden transition is large enough to allow a clear detection in the observed ESR hyperfine structures.

In addition, it has been widely accepted that forbidden hyperfine lines are enhanced in intensity and that their resonant field positions are affected by a combination of the nuclear Zeeman interaction and nuclear quadrupole interaction.<sup>3)</sup> If the magnitudes of the two terms are about the same and sufficiently enough for the detection of a forbidden transition, one

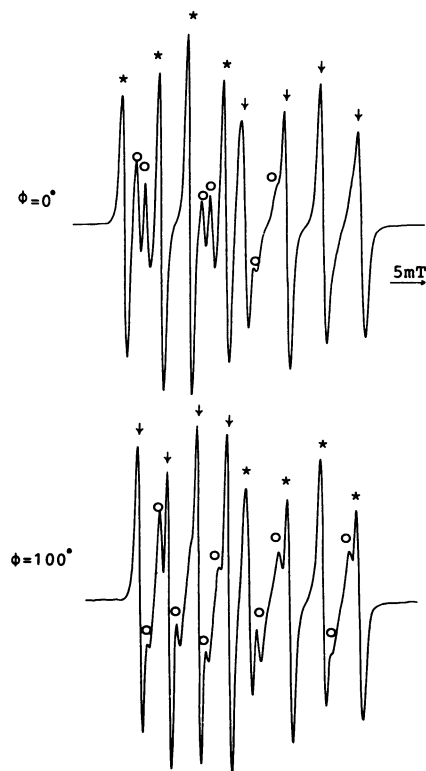


Fig. 3. ESR spectra of  $^{65}\text{Cu}(\text{II})$  doped in the single crystal of B15C5-Mg(II) complex. The temperature of the sample was 77 K and the  $\alpha$  angle was  $2.8^\circ$ . The definition of the  $\alpha$  and  $\phi$  angles are given in Fig. 1. Asterisk and arrow indicate the allowed hyperfine splittings of the sites 1 and 2, respectively. The other spectral lines with open circle are due to the forbidden transitions.

can expect three pairs of forbidden transition lines to occur in middle of the respective allowed  $^{65}\text{Cu}(\text{II})$  hyperfine splittings; that is, the low-, medium-, and high-field pairs of forbidden transitions should be detected at a medium magnetic field, between those of four hyperfine lines of the copper(II) ion. The intensity of the medium-field pair is affected by the nuclear Zeeman term. On the other hand, the nuclear quadrupole term, as well as the nuclear Zeeman term, contribute to the intensity of the low- and high-field pairs, which results in the asymmetry of the observed forbidden hyperfine structure. In the present case, however, the line intensity for each of the low- and high-field pairs is nearly the same, while the intensity for the medium-field pair is greatly reduced in comparison with those of the low- and high-field pairs, as can be seen in Figs. 3 and 4. The contribution of the nuclear quadrupole term to the intensity of the low- and high-field pairs is calculated as to be the same. Therefore, it is suggested that the forbidden transitions mainly arise from a nuclear quadrupole interaction, and that the contribution to the line intensity from the nuclear quadrupole term is rather larger than that from the nuclear Zeeman term in this

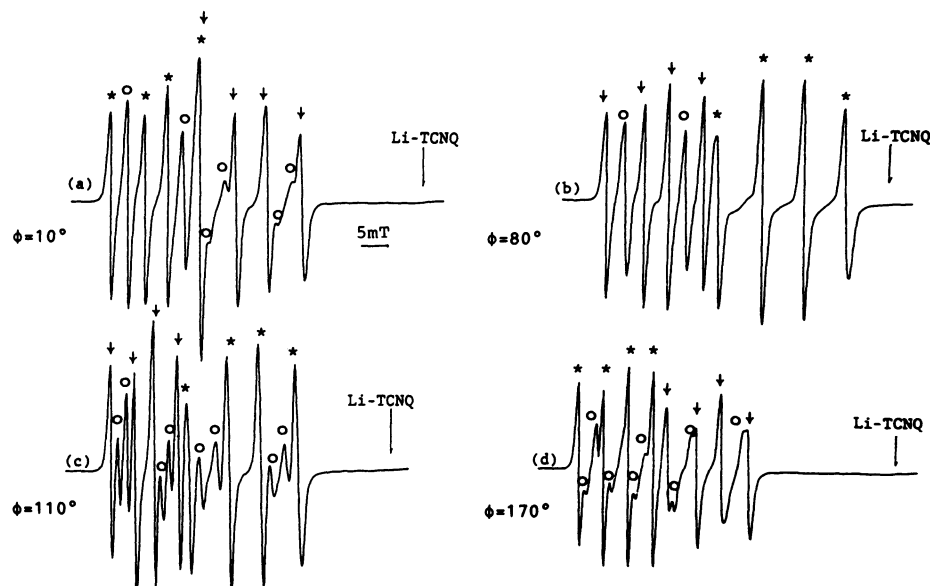


Fig. 4. The angular dependent forbidden ESR spectra of  $^{65}\text{Cu}(\text{II})$  doped in the single crystal of B15C5-Mg(II) complex, which are labeled with open circle. The symbols and the condition in the experiment are the same as those in Fig. 3, except for  $\alpha=18.2^\circ$ .

case.

By taking account of the view described above, an analysis of the single-crystal ESR spectra was performed based on the spin Hamiltonian given by

$$\mathcal{H} = \beta \mathbf{H} \cdot \mathbf{g} \cdot \mathbf{h} + \mathbf{I} \cdot \mathbf{A} \cdot \mathbf{S} + \mathbf{I} \cdot \mathbf{Q} \cdot \mathbf{I},$$

where  $\mathbf{h}$  is a unit vector along the external magnetic field and the other symbols refer to the usual conventions. Within the limits of a high-field approximation, a general solution to the second order has been derived by Iwasaki<sup>4)</sup> for the Hamiltonian in an arbitrary coordinate system without making any assumption that the  $\mathbf{g}$ ,  $\mathbf{A}$ , and  $\mathbf{Q}$  tensors are coaxial. According to the general solution, a computer analysis was carried out for the angular variation of the single crystal ESR spectra.

Figure 5 shows the angular variation of the allowed hyperfine lines of  $^{65}\text{Cu}(\text{II})$  doped in a single-crystal of B15C5-Mg(II). The open and solid circles indicate the observed line positions of the two copper sites. The spin Hamiltonian parameters estimated from the single-crystal ESR study are listed in Table 1. The solid lines in Fig. 5 represent the angular variations calculated based on the spin Hamiltonian parameters.

As shown in Fig. 5, the measured values agree well with the calculated values. At some  $\phi$  angles, the high-field and low-field spacings of the  $^{65}\text{Cu}(\text{II})$  hyperfine splittings are not equal to the medium-field spacing. This has also been realized by means of the quadrupole interaction, since the second-order per-

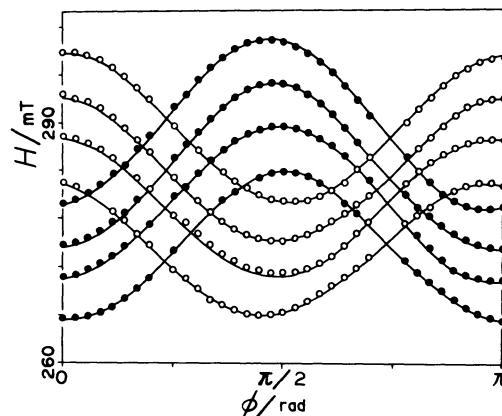


Fig. 5. The angular variation of the allowed hyperfine line positions of  $^{65}\text{Cu}(\text{II})$  doped in the single crystal of B15C5-Mg(II) complex at  $\alpha=2.8^\circ$ . The solid and open circles are of the sites 1 and 2, respectively. The solid lines are the reproduction calculated with the parameters in Table 1.

turbation due to this interaction shifts the respective positions of the four lines.

The simulated powder ESR spectrum based on the same parameters is close to the observed spectrum, as shown in Figs. 2 (a) and (b). This fact confirmed that the copper(II) ion was doped in the single crystal in the form of a B15C5-copper(II) complex. The spin Hamiltonian parameters of the two sites are in agreement within the error limit. Therefore, the two copper(II) sites are in the same ligand field environ-

Table 1. Estimated Principal Values and Axes of  $g$ ,  $A$ , and  $Q$  tensors of B15C5-<sup>65</sup>Cu(II) Complex

Principal value <sup>a)</sup> and (estimated standard deviation)	Direction cosine <sup>b)</sup>			Corresponding parameters in 60%-HClO <sub>4</sub> solution
Site 1 (with * mark in Figs. 3 and 4)				
$g_x$ 2.408(0.002)	0.8333	-0.5034	-0.2282	2.330
$g_y$ 2.296(0.001)	0.2933	0.7527	-0.5894	
$g_z$ 2.030(0.003)	0.4685	0.4242	0.7750	
$A_x$ 5.00(0.03)	0.9462	-0.2420	-0.2147	3.2
$A_y$ 3.00(0.03)	0.0941	0.8409	-0.5330	
$A_z$ 10.39(0.04)	0.3095	0.4841	0.8184	
$Q_x$ -0.51(0.03)	0.7665	-0.5823	-0.2709	11.5
$Q_y$ -0.24(0.03)	0.2573	0.6650	-0.7012	
$Q_z$ 0.71(0.03)	0.5884	0.4678	0.6595	
Site 2 (with arrow mark in Figs. 3 and 4)				
$g_x$ 2.389(0.002)	-0.4595	0.8804	-0.1169	2.330
$g_y$ 2.287(0.003)	0.7458	0.3111	-0.5890	
$g_z$ 2.036(0.007)	0.4822	0.3579	0.7996	
$A_x$ 5.64(0.05)	-0.4301	0.9021	-0.0342	3.2
$A_y$ 2.72(0.06)	0.7632	0.3431	-0.5476	
$A_z$ 10.54(0.09)	0.4822	0.2616	0.8361	
$Q_x$ -0.48(0.05)	-0.2131	0.9701	-0.1164	11.5
$Q_y$ -0.27(0.05)	0.7716	0.0940	-0.6291	
$Q_z$ 0.59(0.05)	0.5993	0.2239	0.7686	

a) Principal values of the  $A$  and  $Q$  tensors are in mT. b) Direction cosines of the principal axis are referred to the (0-123) coordinate system.

Table 2. Relation between Principal Axes of the  $g$ ,  $A$ , and  $Q$  tensors of B15C5-<sup>65</sup>Cu(II) Complex

Between	Angle/deg	
	Site 1	Site 2
$g_x$ and $A_x$	16.4	5.2
$g_y$ and $A_y$	12.9	3.2
$g_z$ and $A_z$	10.1	5.9
<mean>	13.1	4.8
$g_x$ and $Q_x$	6.4	15.1
$g_y$ and $Q_y$	8.4	12.8
$g_z$ and $Q_z$	9.9	10.4
<mean>	8.2	12.7
$A_x$ and $Q_x$	22.4	13.9
$A_y$ and $Q_y$	16.9	15.1
$A_z$ and $Q_z$	18.5	8.1
<mean>	19.3	12.3

ment.

The angles between the estimated principal axes of the  $g$  and  $A$  tensors, and those of  $g$  and  $Q$  tensors, are listed in Table 2. Those values are varied from 3.2° to 16.4° and the simple mean value is 9.7°. In order to determine whether these values are significant or not, the error limit required in the direction cosines is less than 2%. However, the accuracy in the present measurements is not considered enough to do so.

The marked nuclear quadrupole interaction can be attributed to the considerable perturbing effect of the axial ligands on the copper(II) ion with a 3d<sup>9</sup> ground

state in a B15C5-Cu(II) complex,<sup>1,5)</sup> since a strong axial ligation results in a large molecular electric field gradient which interacts with the nuclear electric quadrupole.

In the present paper, the relation between the principal axes of the  $g$ ,  $A$ , and  $Q$  tensors and the crystallographic axes of the single crystal is not discussed, since X-ray structural analysis of the host crystal has not yet been performed.

ESR measurements were carried out at the Advanced Instrumentation Center for Chemical Analysis of this University. The calculations were performed at the Computer Center of this University.

## References

- 1) K. Ishizu, T. Haruta, K. Nakai, K. Miyoshi, and Y. Sugiura, *Chem. Lett.*, **1978**, 579; K. Ishizu, T. Haruta, Y. Kohno, K. Mukai, and Y. Sugiura, *Bull. Chem. Soc. Jpn.*, **53**, 3513 (1980); Y. Li, K. Tajima, K. Ishizu, and N. Azuma, *Bull. Chem. Soc. Jpn.*, **60**, 557 (1987).
- 2) C. J. Pedersen, *J. Am. Chem. Soc.*, **89**, 7017 (1967).
- 3) H. So and R. L. Belford, *J. Am. Chem. Soc.*, **91**, 2392 (1969); L. K. White and R. L. Belford, *J. Am. Chem. Soc.*, **98**, 4428 (1976).
- 4) M. Iwasaki, *J. Magn. Reson.*, **16**, 417 (1974).
- 5) T. Sakurai, K. Kobayashi, S. Tsuboyama, Y. Kohno, N. Azuma, and K. Ishizu, *Acta Crystallogr., Sect. C*, **39**, 206 (1983).